HAL
open science

Technical note: an interannual inversion method for continuous CO2 data

R. M. Law

To cite this version:

R. M. Law. Technical note: an interannual inversion method for continuous CO2 data. Atmospheric Chemistry and Physics Discussions, 2003, 3 (6), pp.5977-6000. hal-00301387

HAL Id: hal-00301387

https://hal.science/hal-00301387v1

Submitted on 18 Jun 2008

HAL is a multi-disciplinary open access archive for the deposit and dissemination of scientific research documents, whether they are published or not. The documents may come from teaching and research institutions in France or abroad, or from public or private research centers.

L'archive ouverte pluridisciplinaire **HAL**, est destinée au dépôt et à la diffusion de documents scientifiques de niveau recherche, publiés ou non, émanant des établissements d'enseignement et de recherche français ou étrangers, des laboratoires publics ou privés.

Atmos. Chem. Phys. Discuss., 3, 5977–6000, 2003
www.atmos-chem-phys.org/acpd/3/5977/
© European Geosciences Union 2003

Atmospheric Chemistry and Physics Discussions

© EGU 2003

Technical note: an interannual inversion method for continuous CO_2 data

R. M. Law

CSIRO Atmospheric Research, Aspendale, Victoria, Australia

Received: 3 October 2003 – Accepted: 18 November 2003 – Published: 21 November 2003

Correspondence to: R. M. Law (rachel.law@csiro.au)

Abstract

A sequential synthesis inversion method is described to estimate CO_2 sources from continuous atmospheric data. The sequential method makes the problem computationally feasible. The method is assessed using four-hourly synthetic concentration data generated from known sources. Multi-year mean sources and seasonal cycles are estimated with comparable quality as those from a traditional inversion of monthly mean data. Interannual variations in the estimated sources are closer to those of the known sources using the four-hourly data rather than monthly data. The computational cost of the basis function simulations can be reduced by generating responses that are only six months long. This does not significantly degrade the inversion results compared to using responses that are 12 months in length.

1. Introduction

There is much information in continuous CO_2 measurements that is currently ignored when estimating CO_2 sources using atmospheric inversions forced with monthly concentration data. A number of studies (e.g. Biraud et al., 2002; Wang and McGregor, 2003) have estimated regional emissions using continuous data from a single site while other studies have explored the development of synthesis inversion methods to incorporate continuous, say hourly, measurements globally (Law et al., 2002, 2003). These methodological tests used synthetic CO_2 data created by an atmospheric transport model from known sources, allowing the retrieved sources to be assessed. However the tests were simplified by using a "cyclo-stationary" inversion method, which assumes that concentration measurements can be averaged over a number of years and estimates mean sources. This assumption is reasonable when using model-generated data with repeating meteorology but for real data, the cyclo-stationary inversion method will no longer be appropriate. Instead, it will be necessary to estimate interannually-varying fluxes and to account for interannually-varying atmospheric transport. Here the

ACPD

3, 5977–6000, 2003

© EGU 2003

first of these two requirements is considered.

2. Method

A Bayesian synthesis inversion method (Rayner et al., 1999) is used, solving for 116 regions and using four-hourly synthetic data for 35 sites for a 17 year period (1981–1997). The four-hourly frequency of the data, rather than the more usual monthly frequency, means that performing a synthesis inversion for the full period is not computationally feasible; the arrays involved are too large. Instead the inversion is run for each year of data separately. We describe this modification to the inversion method shortly.

The basis functions used are monthly pulses from 116 regions. Region boundaries are shown in Fig. 1. The source is emitted uniformally (in space and time) throughout the month of the pulse and the transport model simulation is continued for a further 11 months. Currently we only have access to one year of climate model wind data to force the transport model but for this method to be implemented with real data, it will be necessary to generate response time series for each year of winds, at significant computational cost. Thus it is worth testing how our results are degraded if shorter responses e.g. 3, 6, or 9 months are used.

Bayesian synthesis inversion uses prior information about the sources. Here, prior source estimates and uncertainties are used that are consistent with the protocol for "level 3" of the TransCom3 experiment (http://www.phys.uu.nl/~houwelng/TRANSCOM/t3l3_protocol.htm). The prior sources account for estimates of land-use change. They are typically small and positive for tropical land regions and small and negative for northern mid-latitude land regions and zero elsewhere (including all ocean regions). The TransCom3, level 3 source uncertainties were taken as double those used for the TransCom3 annual mean inversion (Gurney et al., 2002). These are defined for 11 land and 11 ocean regions. These uncertainties are allocated to our smaller regions by weighting the source variance by net primary production for land regions and area for ocean regions. The mean uncertainty for land regions is around 500 $gC\,m^{-2}yr^{-1}$

© EGU 2003

and around 80 gC $m^{-2}yr^{-1}$ for ocean regions. The prior sources and uncertainties are listed for all regions in Table 1.

2.1. Sequential synthesis inversion

The inversion is run in two-year overlapping segments. The steps involved for the case presented here are as follows.

1. For 1981 the inversion is run for a single year and sources are estimated for 1981.

2. The 1982 data are introduced to the inversion, which is run over two years, 1981 and 1982. The 1981 source estimates and uncertainties from step 1 (ignoring any covariance between sources) are used as the prior estimates for 1981 while the 1982 prior estimates are the Transcom3-based ones. The 1982 CO_2 data improve the source estimates for 1981 (because, for example, January concentrations will contain information about December sources). The 1981 data are not used in this second step because data should not be used twice in an estimation.

3. The process is repeated, advancing one year at a time. Each time the two-year inversion uses the source estimates and uncertainties from the previous inversion to provide the prior information for the first year while introducing new concentration data for the second year.

Comparisons between the sequential method and a five year inversion (two years spin-up, three years data, 1993–1995), showed that the sequential method gives very similar sources for all but the final month of the inversion period. For example, the average RMS bias for December 1994 sources from the sequential inversion compared to the five-year inversion was 0.16 GtC yr^{-1} compared to RMS biases of less than 0.04 GtC yr^{-1} for the other months of 1994. Largest biases occurred for regions that are more distant from the data. However, these source estimates are corrected in the next step of the inversion, when the new year of data is introduced. The December 1994

ACPD
3, 5977–6000, 2003

© EGU 2003

RMS bias is reduced from 0.16 to 0.06 GtC yr^{-1} and the November value from 0.04 to 0.03 GtC yr^{-1}. Hence, to reconstruct a full timeseries of fluxes from the two-year overlapping inversions, it is best to retain the source estimates from November year 1 to October year 2. For the final year of the inversion (1997), the year 2 November and December estimates are used to complete the calendar year.

2.2. Data

The synthetic data are created from a forward model run with interannually-varying ocean, biosphere and fossil fluxes. The fossil sources are taken from Andres et al. (1996). The spatial distribution of the fluxes is fixed in time but the magnitude increases to match global emission estimates (Marland and Boden, 1997). The ocean fluxes are from an ocean general circulation model (Le Quéré et al., 2000, 2003) and the biosphere fluxes are from a model driven by observed temperature, precipitation and solar radiation (Friedlingstein et al., 1995). These fluxes have plausible interannual variations and provide an appropriate test for the inversion method. Note that they will not necessarily sum to the known global CO_2 flux inferred from atmospheric concentrations.

The model simulation was sampled four hourly at 35 locations (Fig. 1). These locations are all places where CO_2 is currently sampled (except the central Australian point), though mostly with flask measurements rather than continuously. The higher density of data and smaller regions for Australia provide a best-case example of how the inversion would perform if a larger network of sites was available. The data uncertainty applied to each site depends on the location of the site and ranges from 0.66 ppm for South Pole to 9.30 ppm for Hungary. The values used are twice those prescribed for the TransCom3, level 3 experiment for monthly data. The factor of two is used because most monthly mean data are generated from approximately four, weekly, samples and data uncertainty should scale by $\sqrt{n}$. A full list of data uncertainties is given in Table 2.

© EGU 2003

2.3. Experiments

The sequential synthesis inversion described above is performed using four-hourly data from the full data set of 35 sites. The 1981 source estimates are discarded (as unreliable) and the analysis is performed for 1982–1997. We refer to this inversion as "4HR". For comparison, an inversion using monthly mean data is also performed. For this inversion the data uncertainties prescribed for the TransCom3, level 3 experiment are used and are listed in Table 2. The same prior sources and uncertainties are used as the four-hourly data case. We refer to this inversion as "MON".

In a second set of experiments, the sequential synthesis inversion is repeated but the response functions at the data locations are truncated after 3, 6, and 9 months. The remaining months of the year-long response are manufactured using an exponential decay. Fits to the full 12 month responses at a test site showed that a decay time of approximately 90 days was appropriate, which is substantially shorter than interhemispheric mixing times.

2.4. Measures of inversion quality

To compare the 4HR inversion with the MON inversion, the source estimates for each region are decomposed into the 1982–1997 mean, a mean seasonal cycle (by averaging the same month in all years and subtracting the 1982–1997 mean), and the residual. The residual represents interannual variations (IAV). Both inversions are compared with the known, input sources. For the mean seasonal cycle, we calculate a root mean square bias:

$$\mathrm{RMSB}=\sqrt{\frac{1}{12}\sum_{n=1}^{12}(S_n-F_n)^2} \tag{1}$$

where S_n is the seasonal component of the estimated source for month n and F_n is the seasonal component of the correct source for month n. For the interannual component

© EGU 2003

of the sources, we calculate the correlation between the estimated and correct residual fluxes. This is a measure of the "shape" of the interannual variability. As a measure of the magnitude of the interannual variability, we compare the standard deviation of the estimated and correct residual fluxes.

To assess the inversions using shorter responses (3, 6, 9 months), the source estimates are compared to those using 12 month responses. The root mean square bias for each region is calculated from the full monthly sources for 1982–1997.

3. Results and discussion

3.1. Comparison of 4HR and MON inversions

Figure 1 shows the bias in 1982–1997 source estimates for the two inversions. In both cases the 1982–1997 mean source is estimated to within ±20 $gC\,m^{-2}yr^{-1}$ for all, but one, ocean regions. The biases for land regions are larger especially for the 4HR inversion (only 35% of land regions within ±20 $gC\,m^{-2}yr^{-1}$ compared to 55% for the MON inversion). The larger biases tend to occur for regions without sites nearby. Most of the bias is likely to be due to aggregation errors (Kaminski et al., 2001) caused by the different spatial pattern of sources within a region for the input source and for the basis functions. The aggregation biases appear to be larger with the use of more frequent data (Law et al., 2002).

Figure 2 shows the RMS bias for the estimated mean seasonal cycle. For both inversions, there are larger biases for land regions than ocean regions, as expected since the seasonal cycle of land fluxes is larger than that of the ocean fluxes. Mostly the 4HR inversion gives somewhat better results than the MON inversion. This is noticeable for southern land regions. The 4HR inversion almost always gives better results for regions that include, or are close by, a measuring site.

Figure 3 shows the correlation and Fig. 4 the difference in standard deviation between the interannual component of the estimated and correct sources. The correla-

© EGU 2003

tions are larger for more regions in the 4HR inversion than the MON inversion. For example, in the 4HR inversion 53 regions show correlations greater than 0.6 whereas in the MON inversion only 17 regions show correlations of that magnitude. The magnitude of the variability is also better, for these regions with large correlation, in the 4HR case; the difference in standard deviation is less than ±20 $gC\,m^{-2}yr^{-1}$ for 72% of regions with correlation greater than 0.6 for 4HR compared to only 41% for MON. Mostly the magnitude of the variability is too small in the MON case, particularly for land regions, whereas in the 4HR case southern Africa and South America tend to show variability that is too small while in Eurasia and South-East Asia the variability is too large. In the 4HR case, the lowest correlations are for the tropical Indian ocean and the tropical and south Atlantic ocean, even with data at Seychelles (5° S, 55° E) and Ascension (8° S, 14° W). It is possible that some part of the larger variability on land is misallocated to the nearby ocean regions and "swamps" the ocean variability.

3.2. Other inversion tests with four-hourly data

The sensitivity of the inversion to the prior source uncertainties has been tested by running a case in which the prior source uncertainty is halved. Overall there are only small differences in the source estimates. The differences in the 1982–1997 mean tend to move the solution closer to the correct sources for most regions. Changes in correlation are small with positive differences for about 60% of the regions. The magnitude of the interannual variability is reduced as expected, given the smaller prior source uncertainty. This improves the variability for those regions that were originally overestimated (Eurasia) but degrades it for those regions that were underestimated (southern Africa and South America).

To investigate the idea that ocean variability is masked by misallocation of land variability, an inversion is performed using synthetic data generated from the ocean fluxes only. For ocean regions, there are small improvements in the 1982–1997 mean results and the mean seasonal cycle. IAV correlations for the ocean regions improve markedly; 25 regions show correlations greater than 0.6 compared to only 15 previously and 17

© EGU 2003

of these are above 0.7 compared to only seven previously. The improvements are especially noticeable in the tropical and northern Atlantic and in the tropical Indian ocean (though the correlations remain low around the Bay of Bengal). There is little change in the magnitude of interannual variability. This result supports the idea that ocean IAV is masked by misallocated land IAV. It is not clear what the solution to this is, given that in the real world, we cannot measure "ocean-only" concentrations. A higher density of observing sites may minimise the problem.

3.3. Comparison of inversions with shorter responses

Figure 5 shows the RMS difference in total source (calculated across all months from 1982–1997) between the 4HR inversion using 12 month responses and inversions using 3, 6 and 9 month responses. Also shown is the RMS difference between the 4HR inversion and the correct sources. This provides a benchmark against which to assess the differences due to changing the response length. As expected the differences from the 12 month case decrease as the response length increases. The largest RMS differences occur mostly for the land regions that do not have a site nearby: central Eurasia, tropical Africa, South America and tropical Asia. In the 3 month case, the largest differences are comparable to the differences between the 12 month sources and the correct sources. This suggests that using a response length of only 3 months may compromise the inversion results. In the 6 month case, the RMS differences are smaller than the benchmark. Thus, if computational resources are limited, it would appear that 6 month responses could be used and an adequate inversion still obtained.

4. Conclusions

The inversion results presented here have shown that continuous CO_2 measurements could be used to estimate sources with relatively small changes to the current inversion techniques used with monthly mean data. The size of the inversion can be made

© EGU 2003

feasible by running sequentially in two-year overlapping time intervals. The cpu time required to generate the response functions can be reduced by only running the atmospheric transport model for six months and approximating the rest of the response with an exponential decay. In the tests performed here, better results were generally achieved using the continuous data than using monthly data, especially for interannual variations. Aggregation biases continue to be seen in the multi-year mean results, suggesting the need for smaller regions in the inversion set-up. Future work is required to repeat these tests using a transport model capable of using analysed (and consequently interannually varying) winds. We can then begin to invert real continuous data.

Acknowledgements. C. Trudinger and P. Rayner provided useful comments on the manuscript.

References

Andres, R. J., Marland, G., Fung, I., and Matthews, E.: A 1°×1° distribution of carbon dioxide emissions from fossil fuel consumption and cement manufacture, 1950–1990, Global Biogeochem. Cycles, 10, 419–429, 1996. 5981

Biraud, S., Ciais, P., Ramonet, M., Simmonds, P., Kazan, V., Monfray, P., O'Doherty, S., Spain, G., and Jennings, S. G.: Quantification of carbon dioxide, methane, nitrous oxide and chloroform emissions over Ireland from atmospheric observations at Mace Head, Tellus, 54B, 41–60, 2002. 5978

Friedlingstein, P., Fung, I., Holland, E., John, J., Brasseur, G., Erickson, D., and Schimel, D.: On the contribution of CO_2 fertilization to the missing biospheric sink, Global Biogeochem. Cycles, 9, 541–556, 1995. 5981

Gurney, K. R., Law, R. M., Denning, A. S., Rayner, P. J., Baker, D., Bousquet, P., Bruhwiler, L., Chen, Y.-H., Ciais, P., Fan, S., Fung, I. Y., Gloor, M., Heimann, M., Higuchi, K., John, J., Maki, T., Maksyutov, S., Masarie, K., Peylin, P., Prather, M., Pak, B. C., Randerson, J., Sarmiento, J., Taguchi, S., Takahashi, T., and Yuen, C.-W.: Towards robust regional estimates of CO_2 sources and sinks using atmospheric transport models, Nature, 415, 626–630, 2002. 5979

© EGU 2003

Kaminski, T., Rayner, P. J., Heimann, M., and Enting, I. G.: On aggregation errors in atmospheric transport inversions, J. Geophys. Res., 106, 4703–4715, 2001. 5983

Law, R. M., Rayner, P. J., Steele, L. P., and Enting, I. G.: Using high temporal frequency data for CO_2 inversions, Global Biogeochem. Cycles, 16, 1053, doi:10.1029/2001GB001593, 2002. 5978, 5983

Law, R. M., Rayner, P. J., Steele, L. P., and Enting, I. G.: Data and modelling requirements for CO_2 inversions using high frequency data, Tellus, 55B, 512–521, doi:10.1034/j.1600-0560.2003.0029.x, 2003. 5978

Le Quéré, C., Orr, J. C., Monfray, P., Aumont, O., and Madec, G.: Interannual variability of the oceanic sink of CO_2 from 1979 through 1997, Global Biogeochem. Cycles, 14, 1247–1265, 2000. 5981

Le Quéré, C., Aumont, O., Bopp, L., Bousquet, P., Ciais, P., Francey, R., Heimann, M., Keeling, C. D., Keeling, R. F., Kheshgi, H., Peylin, P., Piper, S. C., Prentice, I. C., and Rayner, P. J.: Two decades of ocean CO_2 sink and variability, Tellus, 55B, 649–656, doi:10.1034/j.1600-0560.2003.00043.x, 2003. 5981

Marland, G. and Boden, T.: Estimates of global, regional, and national annual CO_2-emissions from fossil-fuel burning, hydraulic cement production, and gas flaring: 1950–1994, NDP-030R7, Carbon Dioxide Information Analysis Center, Oak Ridge National Laboratory, 1997. 5981

Rayner, P. J., Enting, I. G., Francey, R. J., and Langenfelds, R. L.: Reconstructing the recent carbon cycle from atmospheric CO_2, $\delta^{13}C$ and O_2/N_2 observations, Tellus, 51B, 213–232, 1999. 5979

Wang, Y.-P. and McGregor, J. L.: Estimating regional terrestrial carbon fluxes for the Australian continent using a multiple-constraint approach. II. The atmospheric constraint, Tellus, 55B, 290–304, doi:10.1034/j.1600-0560.2003.00030.x, 2003. 5978

© EGU 2003

Table 1. Prior source and uncertainty for each region. The regions are labelled by number in Fig. 6.

Region number	type	longitude of region centre (°)	latitude of region centre (°)	prior source uncertainty ($gC\,m^{-2}yr^{-1}$)	prior source uncertainty ($gC\,m^{-2}yr^{-1}$)
1	land	−155.2	64.5	0.0	407.9
2	land	−122.5	66.1	0.0	277.2
3	land	−84.4	67.1	0.0	161.6
4	land	−119.8	56.6	0.0	376.2
5	land	−82.0	53.3	0.0	283.3
6	land	−114.0	45.3	−39.5	567.8
7	land	−87.8	43.7	−65.0	655.6
8	land	−111.0	33.4	−23.2	466.5
9	land	−93.8	31.3	−73.3	594.1
10	land	−74.7	6.2	52.5	532.4
11	land	−57.9	2.5	65.3	699.7
12	land	−71.4	−9.8	44.5	510.5
13	land	−54.5	−9.5	47.5	435.8
14	land	−41.8	−11.8	0.0	851.6
15	land	−64.7	−27.9	0.0	527.6
16	land	−52.1	−24.5	0.0	657.3
17	land	−69.8	−43.5	0.0	446.0
18	land	2.7	24.3	1.2	85.0
19	land	28.4	22.5	0.8	100.3
20	land	4.9	8.5	16.9	435.5
21	land	33.5	7.1	14.6	386.7
22	land	19.0	−7.8	21.6	678.5
23	land	33.0	−8.7	18.8	571.3
24	land	19.9	−24.5	4.9	367.7
25	land	30.0	−23.7	12.5	644.7
26	land	45.0	−20.9	17.2	1298.5

ACPD
3, 5977–6000, 2003

© EGU 2003

Table 1. Continued.

Region number	type	longitude of region centre (°)	latitude	prior source ($gC\,m^{-2}yr^{-1}$)	prior uncertainty
27	land	80.8	66.1	−24.6	447.0
28	land	116.6	66.8	−25.0	433.7
29	land	158.0	64.7	−16.8	381.8
30	land	80.2	53.7	−24.7	453.5
31	land	120.7	52.1	−36.2	459.9
32	land	45.6	36.8	10.6	379.2
33	land	72.7	43.0	6.7	280.6
34	land	106.3	42.0	11.5	342.9
35	land	48.7	23.3	1.6	133.5
36	land	73.1	30.7	10.5	354.3
37	land	104.1	30.7	26.0	508.8
38	land	137.8	36.3	41.9	2310.2
39	land	78.8	19.0	23.7	719.0
40	land	100.7	21.8	134.2	528.4
41	land	104.1	14.0	155.4	879.1
42	land	101.2	0.0	233.7	1501.9
43	land	115.3	0.0	275.4	1153.0
44	land	142.5	−6.0	236.4	1236.9
45	land	121.5	−21.5	0.0	281.7
46	land	120.9	−27.9	0.0	373.9
47	land	120.0	−33.0	0.0	612.1
48	land	133.1	−14.4	0.0	602.4
49	land	132.2	−19.5	0.0	325.5
50	land	132.2	−25.1	0.0	317.5
51	land	133.1	−30.2	0.0	380.4
52	land	143.4	−19.5	0.0	533.4
53	land	143.4	−25.1	0.0	475.6

© EGU 2003

Table 1. Continued.

Region number	type	longitude of region centre (°)	latitude	prior source ($gC\,m^{-2}yr^{-1}$)	prior uncertainty
54	land	143.4	−30.7	0.0	505.0
55	land	144.4	−35.8	0.0	1032.6
56	land	151.9	−29.3	0.0	857.6
57	land	174.4	−40.5	0.0	2414.2
58	land	23.6	63.2	−7.1	572.7
59	land	48.8	62.5	−6.9	589.8
60	land	3.6	47.4	−13.9	709.1
61	land	24.9	48.1	−13.0	652.7
62	land	47.5	50.1	−6.9	529.8
63	land	16.9	79.5	0.0	567.4
64	ocean	161.9	50.9	0.0	91.2
65	ocean	−153.7	51.2	0.0	84.1
66	ocean	149.8	27.0	0.0	50.7
67	ocean	−143.4	26.9	0.0	50.0
68	ocean	123.3	6.1	0.0	67.4
69	ocean	171.6	5.6	0.0	55.0
70	ocean	172.1	−9.8	0.0	61.2
71	ocean	−137.8	5.6	0.0	66.5
72	ocean	−96.8	5.4	0.0	73.8
73	ocean	−137.8	−9.8	0.0	73.2
74	ocean	−96.6	−10.0	0.0	80.6
75	ocean	175.4	−23.5	0.0	139.3
76	ocean	−137.8	−23.7	0.0	144.5
77	ocean	−92.8	−23.7	0.0	144.5
78	ocean	174.9	−37.7	0.0	149.9
79	ocean	−137.8	−37.7	0.0	155.4
80	ocean	−94.4	−37.4	0.0	161.3

© EGU 2003

Table 1. Continued.

Region number	type	longitude of region centre (°)	latitude	prior source ($gC\,m^{-2}yr^{-1}$)	prior uncertainty
81	ocean	135.6	75.4	0.0	38.5
82	ocean	−58.1	59.4	0.0	56.0
83	ocean	−8.4	60.3	0.0	54.0
84	ocean	−61.1	38.9	0.0	72.0
85	ocean	−27.2	40.7	0.0	56.0
86	ocean	−71.1	22.6	0.0	51.7
87	ocean	−30.4	22.5	0.0	59.5
88	ocean	17.6	36.3	0.0	8.0
89	ocean	43.1	43.7	0.0	23.8
90	ocean	−84.4	46.0	0.0	148.5
91	ocean	−37.6	6.7	0.0	59.6
92	ocean	−2.8	1.4	0.0	117.5
93	ocean	−25.3	−9.8	0.0	91.7
94	ocean	0.0	−9.8	0.0	82.0
95	ocean	−29.4	−24.0	0.0	98.5
96	ocean	0.0	−23.7	0.0	102.2
97	ocean	−36.8	−38.1	0.0	87.2
98	ocean	2.8	−37.7	0.0	100.4
99	ocean	84.4	−50.2	0.0	113.3
100	ocean	−141.2	−50.3	0.0	109.4
101	ocean	−22.5	−50.2	0.0	140.4
102	ocean	81.3	−61.6	0.0	130.1
103	ocean	−139.1	−65.6	0.0	101.8
104	ocean	−24.7	−65.1	0.0	139.2
105	ocean	60.9	9.2	0.0	91.7
106	ocean	88.2	7.7	0.0	115.8

© EGU 2003

Table 1. Continued.

Region number	type	longitude of region centre (°)	latitude	prior source ($gC\,m^{-2}yr^{-1}$)	prior uncertainty
107	ocean	57.8	−9.5	0.0	108.4
108	ocean	107.3	−9.7	0.0	82.7
109	ocean	55.9	−24.2	0.0	82.9
110	ocean	96.3	−23.6	0.0	80.4
111	ocean	48.8	−37.9	0.0	75.1
112	ocean	108.9	−38.3	0.0	69.7
113	land	−66.4	77.3	0.0	22.4
114	land	−39.8	77.1	0.0	33.2
115	land	−32.0	72.2	0.0	21.2
116	land	−16.9	65.6	0.0	249.3

ACPD
3, 5977–6000, 2003

© EGU 2003

Table 2. Sites used in the inversion and the data uncertainty applied to the data for each site for the 4HR and MON inversions.

Site	Longitude	Latitude	Data uncertainty (ppm) 4HR	MON
Alert	-62.5	82.5	1.52	0.76
Amsterdam Is	77.5	−38.0	0.84	0.42
Ascension Is	−14.4	−7.9	1.32	0.66
Azores	−27.1	38.8	2.40	1.20
Baring Head	174.9	−41.4	0.78	0.39
Barrow	−156.6	71.3	2.36	1.18
Bermuda West	−64.9	32.3	2.84	1.42
Cape Ferguson	147.1	−19.3	1.70	0.85
Cape Grim	144.7	−40.7	0.70	0.35
Cape Meares	−124.0	45.5	3.50	1.75
Central Aus	135.0	−20.9	1.60	0.80
Christmas Is	−157.2	1.7	0.92	0.46
Cold Bay	−162.7	55.2	2.28	1.14
Darwin	130.6	−12.4	3.52	1.76
Guam	144.8	13.4	1.46	0.73
Halley Bay	−25.5	−75.7	0.64	0.32
Hungary	16.7	47.0	9.30	4.65
Key Biscayne	−80.2	25.7	5.04	2.52
Kumakahi	−154.8	19.5	1.52	0.76
Mace Head	−10.0	52.0	2.24	1.12
Midway	−177.4	28.2	1.80	0.90
Mould Bay	−119.4	76.3	1.66	0.83
Mt Cimone	10.7	44.2	3.76	1.88
Mt Waliguan	100.9	36.3	2.60	1.30
Palmer	−64.0	−64.9	0.70	0.35
Ragged Pt	−59.4	13.2	1.14	0.57
Ryori	141.8	39.0	4.24	2.12

ACPD
3, 5977–6000, 2003

© EGU 2003

Table 2. Continued.

Site	Longitude	Latitude	Data uncertainty (ppm) 4HR	MON
Samoa	−170.6	14.3	1.06	0.53
Schauinsland	8.0	48.0	4.16	2.08
Seychelles	55.2	−4.7	1.58	0.79
Shemya	174.1	52.7	1.82	0.91
South Pole	−24.8	−90.0	0.66	0.33
Station M	2.0	66.0	3.36	1.68
Tae-ahn Pen	126.1	36.7	5.04	2.52
Ulaan Uul	111.1	44.5	2.96	1.48

© EGU 2003

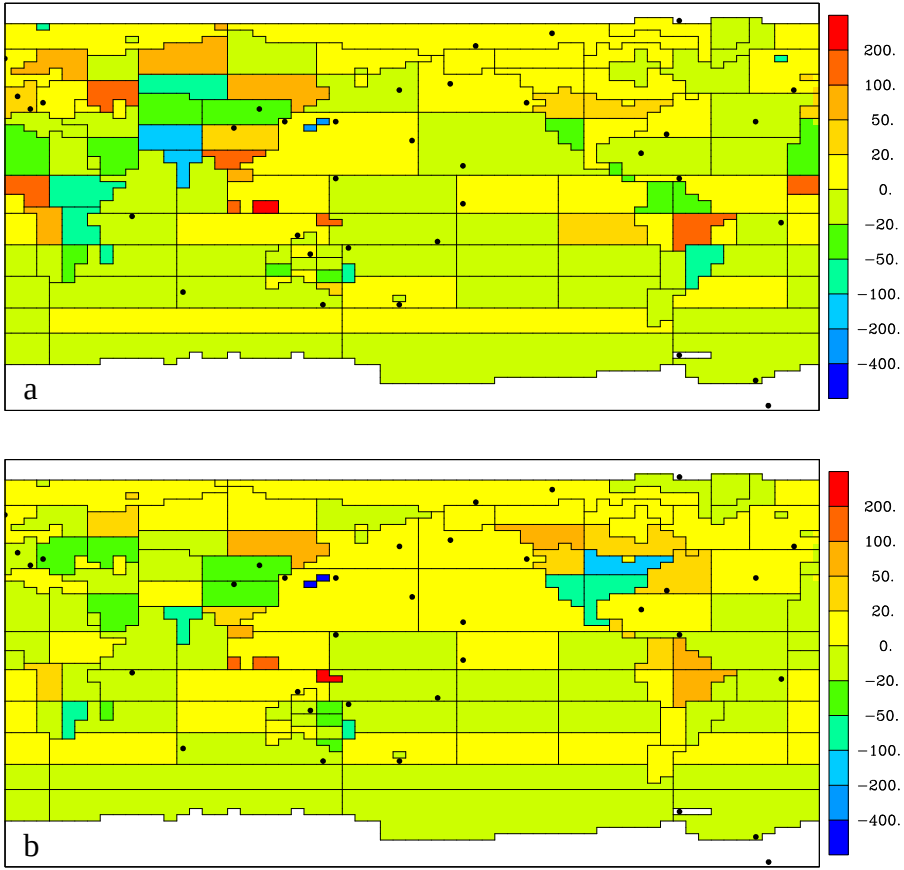

Fig. 1. Bias in 1982–1997 mean source for **(a)** the 4HR inversion and **(b)** the MON inversion. The bias is defined as the difference between the estimated sources and the correct sources. The units are $gC\,m^{-2}yr^{-1}$. The dots indicate the locations of the sampling sites and the lines indicate the region boundaries.

ACPD
3, 5977–6000, 2003

© EGU 2003

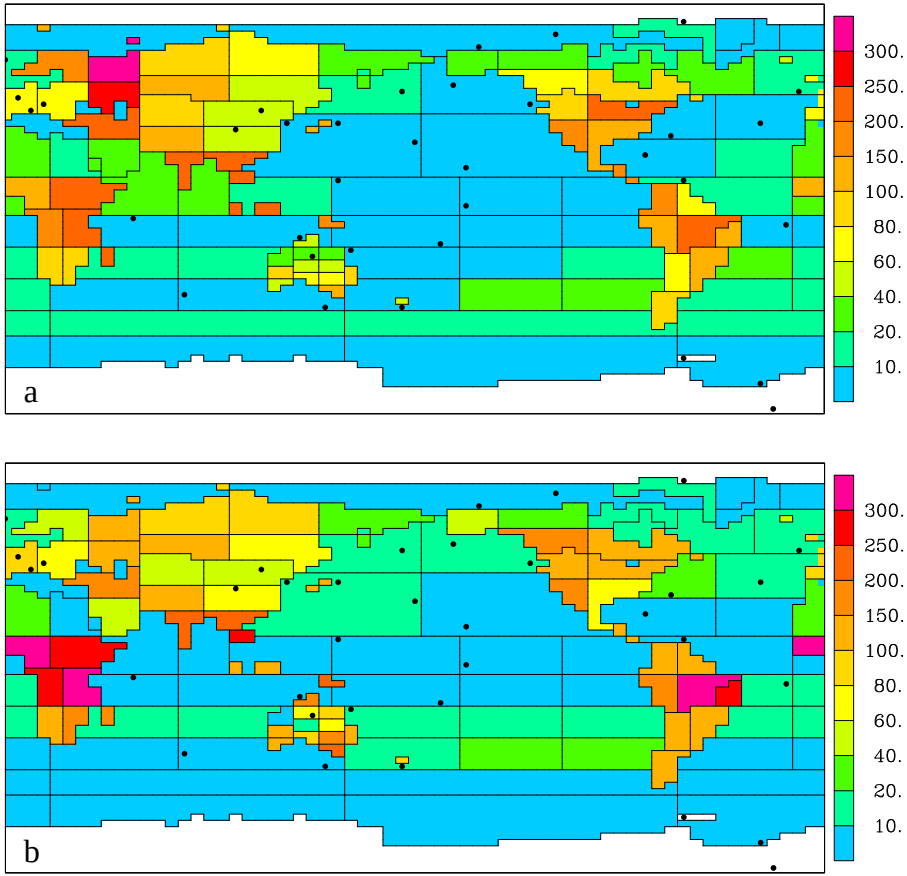

Fig. 2. Root mean square bias in the mean seasonal cycle of sources between the **(a)** 4HR and **(b)** MON inversion results and the correct sources. The units are gC $m^{-2}yr^{-1}$.

ACPD
3, 5977–6000, 2003

Interannual CO_2 inversion method

R. M. Law

© EGU 2003

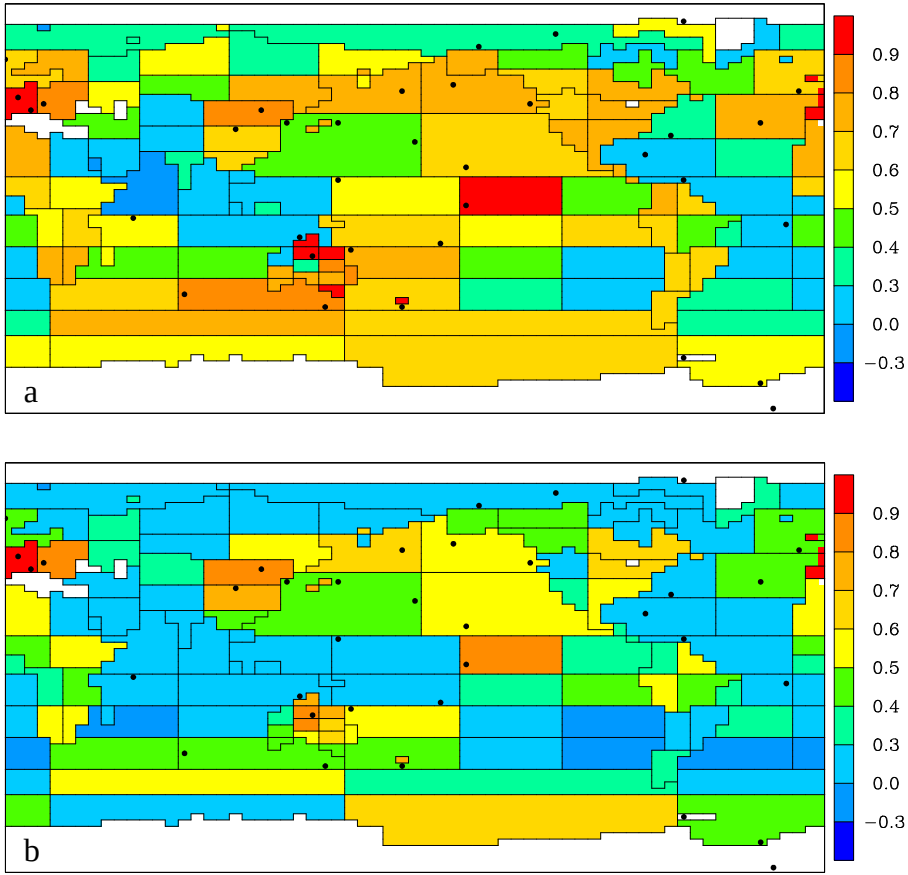

Fig. 3. Correlation between estimated and correct residual sources for **(a)** 4HR and **(b)** MON inversions.

ACPD
3, 5977–6000, 2003

Interannual CO_2 inversion method

R. M. Law

© EGU 2003

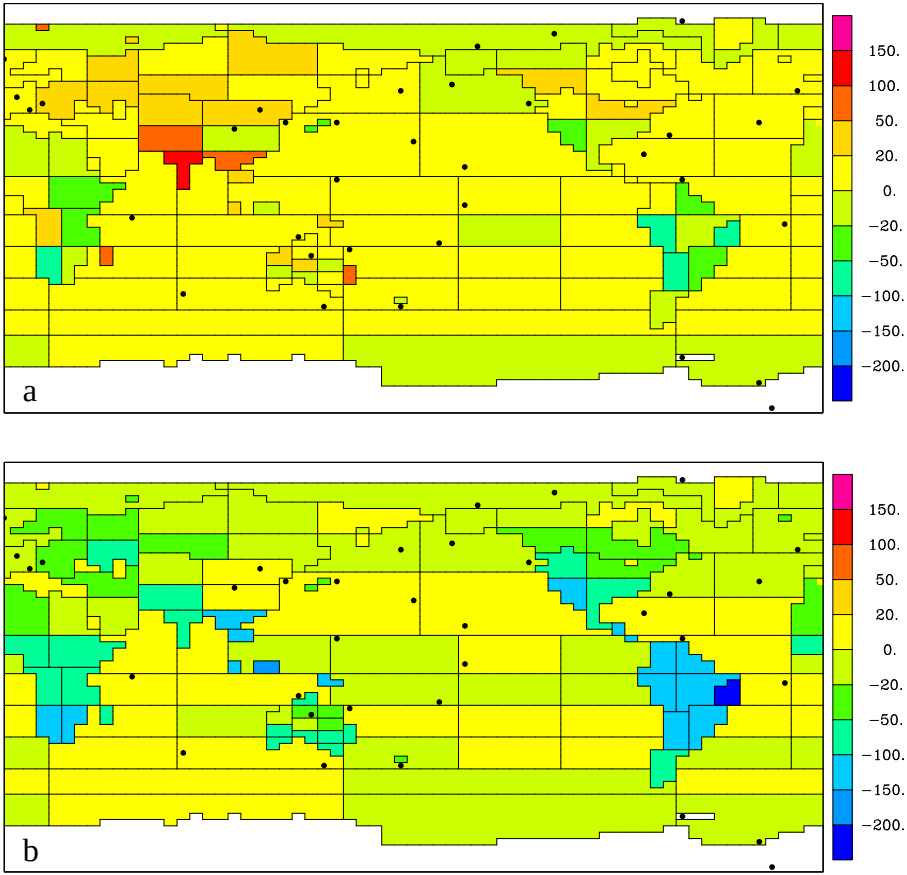

Fig. 4. Difference in standard deviation of estimated and correct residual sources for **(a)** 4HR and **(b)** MON inversions. The units are gC $m^{-2}yr^{-1}$.

ACPD
3, 5977–6000, 2003

© EGU 2003

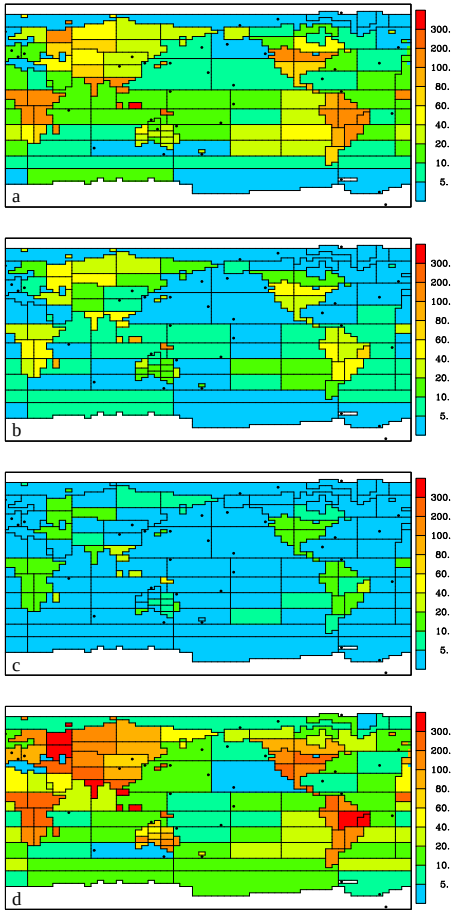

Fig. 5. Root mean square difference in source between inversion results using **(a)** 3 month, **(b)** 6 month, **(c)** 9 month responses and that using 12 month responses and **(d)** between inversion results using 12 month responses and the correct sources. The units are gC $m^{-2}yr^{-1}$.

ACPD
3, 5977–6000, 2003

© EGU 2003

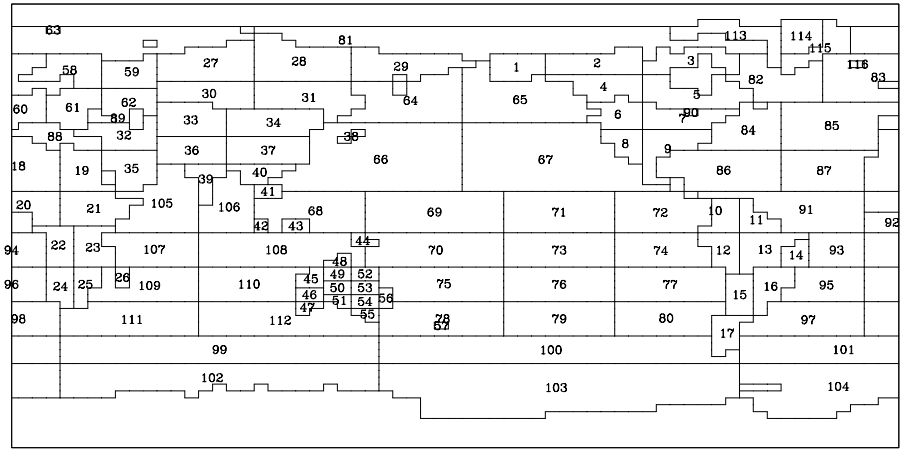

Fig. 6. Map of regions.

ACPD

3, 5977–6000, 2003

Interannual CO_2 inversion method

R. M. Law

© EGU 2003